

12-2022

Data Supporting the Roles of BAP1, Sting, and IFN- β in ISGF3 Activation in ccRCC

Lauren E Langbein
Thomas Jefferson University

Eleonora Sementino
Fox Chase Cancer Center

Zhijiu Zhong
Thomas Jefferson University

Wei Jiang
Thomas Jefferson University

Li Li

Follow this and additional works at: <https://jdc.jefferson.edu/pacbfp>
Thomas Jefferson University

 Part of the [Medical Anatomy Commons](#), [Medical Cell Biology Commons](#), and the [Medical Pathology Commons](#)

See next page for additional authors

[Let us know how access to this document benefits you](#)

Recommended Citation

Langbein, Lauren E; Sementino, Eleonora; Zhong, Zhijiu; Jiang, Wei; Li, Li; Testa, Joseph R; and Yang, Haifeng, "Data Supporting the Roles of BAP1, Sting, and IFN- β in ISGF3 Activation in ccRCC" (2022). *Department of Pathology, Anatomy, and Cell Biology Faculty Papers*. Paper 373.
<https://jdc.jefferson.edu/pacbfp/373>

This Article is brought to you for free and open access by the Jefferson Digital Commons. The Jefferson Digital Commons is a service of Thomas Jefferson University's [Center for Teaching and Learning \(CTL\)](#). The Commons is a showcase for Jefferson books and journals, peer-reviewed scholarly publications, unique historical collections from the University archives, and teaching tools. The Jefferson Digital Commons allows researchers and interested readers anywhere in the world to learn about and keep up to date with Jefferson scholarship. This article has been accepted for inclusion in Department of Pathology, Anatomy, and Cell Biology Faculty Papers by an authorized administrator of the Jefferson Digital Commons. For more information, please contact: JeffersonDigitalCommons@jefferson.edu.

Authors

Lauren E Langbein, Eleonora Sementino, Zhijiu Zhong, Wei Jiang, Li Li, Joseph R Testa, and Haifeng Yang



Data Article

Data supporting the roles of BAP1, STING, and IFN- β in ISGF3 activation in ccRCC

Lauren E. Langbein^a, Eleonora Sementino^b, Zhijiu Zhong^c,
Wei Jiang^a, Li Li^a, Joseph R. Testa^b, Haifeng Yang^{a,*}

^aDepartment of Pathology, Anatomy, & Cell Biology, Thomas Jefferson University, Philadelphia, PA, United States

^bCancer Signaling and Epigenetics Program, Fox Chase Cancer Center, Philadelphia, PA, United States

^cSidney Kimmel Cancer Center, Thomas Jefferson University, Philadelphia, PA, United States

ARTICLE INFO

Article history:

Received 12 September 2022

Revised 26 October 2022

Accepted 7 November 2022

Available online 11 November 2022

Dataset link: [Data supporting the roles of BAP1, STING, and IFN- \$\beta\$ in ISGF3 activation in ccRCC \(Original data\)](#)

Keywords:

Kidney cancer

Type I interferon

BAP1

Tumor suppressor genes

Therapeutic

ABSTRACT

The data presented in this article are companion materials to our manuscript titled “BAP1 maintains HIF-dependent interferon beta induction to suppress tumor growth in clear cell renal cell carcinoma” (Langbein et al., 2022), where we investigated the downstream effects of BAP1 (BRCA1-associated protein 1) expression in clear cell renal cell carcinoma (ccRCC) cell lines and mouse xenograft models. In the manuscript, we showed that BAP1 upregulates STING (stimulator of interferon genes) expression and activity in ccRCC cells, leading to IFN- β transcription and activation of interferon stimulated gene factor 3 (ISGF3), the transcription factor that mediates the effects of type I interferons (IFNs). Here, we suppressed additional components of the type I IFN pathway, including IRF9 (a component of ISGF3), IFNAR1 (the type I IFN receptor), and STING (a stimulator of IFN production) by shRNA to investigate their involvement in BAP1-mediated upregulation of ISGF3 activity. We also inhibited extracellular IFN- β via neutralizing antibody treatment in BAP1-expressing cells to ascertain the role of the secreted cytokine in this pathway. ISGF3 activity was assessed by western blot analysis and qPCR measurement of its transcriptional targets. To examine the relevance of our observations in an-

DOI of original article: [10.1016/j.canlet.2022.215885](https://doi.org/10.1016/j.canlet.2022.215885)

* Corresponding author.

E-mail address: haifeng.yang@jefferson.edu (H. Yang).

Social media: [@Lauren_Langbein](#) (L.E. Langbein), [@yang_haifeng](#) (H. Yang)

<https://doi.org/10.1016/j.dib.2022.108743>

2352-3409/© 2022 The Authors. Published by Elsevier Inc. This is an open access article under the CC BY-NC-ND license (<http://creativecommons.org/licenses/by-nc-nd/4.0/>)

other model system, we characterized primary kidney cells from WT and *Bap1^{fl/fl}* mice by cytokeratin 8 immunohistochemistry and examined the effect of *Bap1* knockout on Sting protein expression. Finally, we treated mice bearing BAP1 knockdown xenografted tumors with diABZI, a STING agonist, and measured immune cell recruitment via CD45 immunohistochemistry. These data can serve as a starting point for further investigation on the roles of BAP1 and other tumor suppressor genes in interferon pathway regulation.

© 2022 The Authors. Published by Elsevier Inc.

This is an open access article under the CC BY-NC-ND license (<http://creativecommons.org/licenses/by-nc-nd/4.0/>)

Specifications Table

Subject	Cancer Research
Specific subject area	Type I interferon pathway stimulation by BAP1 in clear cell renal cell carcinoma
Type of data	Image Graph Figure
How the data were acquired	Western blots: ImageQuant LAS 4000 qPCR: StepOnePlus or QuantStudio 3 Real-Time PCR System IHC: IntelliPATH FLX Autostainer
Data format	Raw Analyzed
Description of data collection	Stable ccRCC cell lines were generated to genetically manipulate factors of interest. Cells were treated with the indicated compounds. Protein lysates were harvested from cells and used in western blots to investigate pathway activity. RNA was extracted from cells, reverse transcribed, and used in qPCR for ISGF3 target genes. Gene expression was calculated using the $\Delta\Delta C_t$ method. Immunohistochemistry was performed on cultured cells derived from WT or <i>Bap1^{fl/fl}</i> mouse kidneys or Ren-02 xenografted tumors. Experiments were performed a minimum of two times.
Data source location	<i>Institution:</i> Thomas Jefferson University <i>City/Town/Region:</i> Philadelphia, PA <i>Country:</i> USA
Data accessibility	Repository name: Mendeley Data Data identification number: 10.17632/nd7vbzyvt6.3 Direct URL to data: https://data.mendeley.com/datasets/nd7vbzyvt6/3
Related research article	L.E. Langbein, R. El Hajjar, S. He, E. Sementino, Z. Zhong, W. Jiang, B.E. Leiby, L. Li, R.G. Uzzo, J.R. Testa, H. Yang, BAP1 maintains HIF-dependent interferon beta induction to suppress tumor growth in clear cell renal cell carcinoma, <i>Cancer Lett.</i> 547 (2022) 215885. doi: 10.1016/j.canlet.2022.215885

Value of the Data

- These data can aid in deciphering the molecular mechanisms of tumor suppression by BAP1 in ccRCC and possibly other cancers.
- Researchers and clinicians working to understand the mechanisms underlying ccRCC pathology and tumor progression can benefit from these data.
- These data can be used to support the development of type I interferon pathway therapeutics for BAP1-deficient ccRCC.

1. Objective

The objective of these data is to expand and strengthen the findings in our primary research article, BAP1 maintains HIF-dependent interferon beta induction to suppress tumor growth in clear cell renal cell carcinoma, published in Cancer Letters. These data provide additional molecular insight into the mechanism of type I IFN pathway activation by BAP1, a tumor suppressor gene implicated in ccRCC and other cancers. Data presented here investigate the involvement of other components in this pathway, including: ISGF3, a heterotrimeric transcription factor that promotes interferon stimulated gene expression; the interferon α receptor (IFNAR), which binds type I IFN to initiate signaling in target cells; secreted IFN- β , a type I IFN cytokine produced in response to pathogens and abnormal host nucleic acids; and STING, an upstream stimulator of type I IFN production.

2. Data Description

2.1. ISGF3 activity is elevated in BAP1-expressing cells

We have previously shown that BAP1 increases the expression of ISGF3 target genes in ccRCC cell lines [1,2]. We wanted to see whether the upregulation of these interferon sensitive genes (i.e. ISGF3 targets) is ISGF3-dependent in cells that express BAP1. We generated UMRC6 ccRCC cells, which lack endogenous BAP1, that express a control vector (GFP) or BAP1. We then knocked down the expression of IRF9, an essential component of ISGF3, using two shRNAs in these cell lines. BAP1, IRF9, and ISGF3 target expression was examined by western blotting. While BAP1 expression increased the abundance of ISGF3 targets STAT2, OAS1, and PLSCR1, IRF9 knockdown reduced this effect in these cells (Fig. 1A). Minimal differences in ISGF3 target levels were seen in the GFP-expressing cells.

Our previous work suggests BAP1 enhances STAT2 phosphorylation in ccRCC cells. Typically, both STAT1 and STAT2 are phosphorylated by Janus kinases (JAK) on the cytoplasmic side of the IFNAR upon IFN binding. To examine whether STAT2 phosphorylation was related to JAK activity, UMRC6 cells expressing GFP or BAP1 were treated with increasing doses of ruxolitinib, a JAK1/2 inhibitor, or IFN- α as a positive control. IFN- α treated cells had high levels of phosphorylated STAT1 and STAT2. BAP1-expressing cells demonstrated increased STAT1 and STAT2 phosphorylation compared to GFP-expressing cells in untreated conditions. Ruxolitinib treatment abolished the elevated phosphorylation of STAT1 and STAT2 in BAP1-expressing cells (Fig. 1B).

2.2. IFN- β treatment increases ISGF3 target levels in IFNB1 knockdown cells

Our previous data show that IFN- β knockdown reduces ISGF3 target levels in BAP1-expressing cells [1]. We examined whether this was indeed due to *IFNB1* suppression, and not an off-target effect of the shRNA. Control (scrambled shRNA, SCR) and *IFNB1* knockdown cells were generated using Ren-02 (ccRCC, BAP1⁺) and UMRC6 GFP- and BAP1-expressing cells. The cells were treated with increasing doses of exogenous recombinant human IFN- β , and ISGF3 target levels were measured by qPCR. *IFNB1* shRNA led to decreased expression of various ISGF3 target genes, including *OAS2*, *IFI44L*, *IRF9*, *OAS1*, and *EPSTI1* in both cell lines. IFN- β treatment increased ISGF3 target expression in both SCR and *IFNB1* knockdown cells in Ren-02 (Fig. 2A) and UMRC6 cells (Fig. 2B, C). Thus, the reduced expression of ISGF3 targets after *IFNB1* suppression was reversed by exogenous IFN- β .

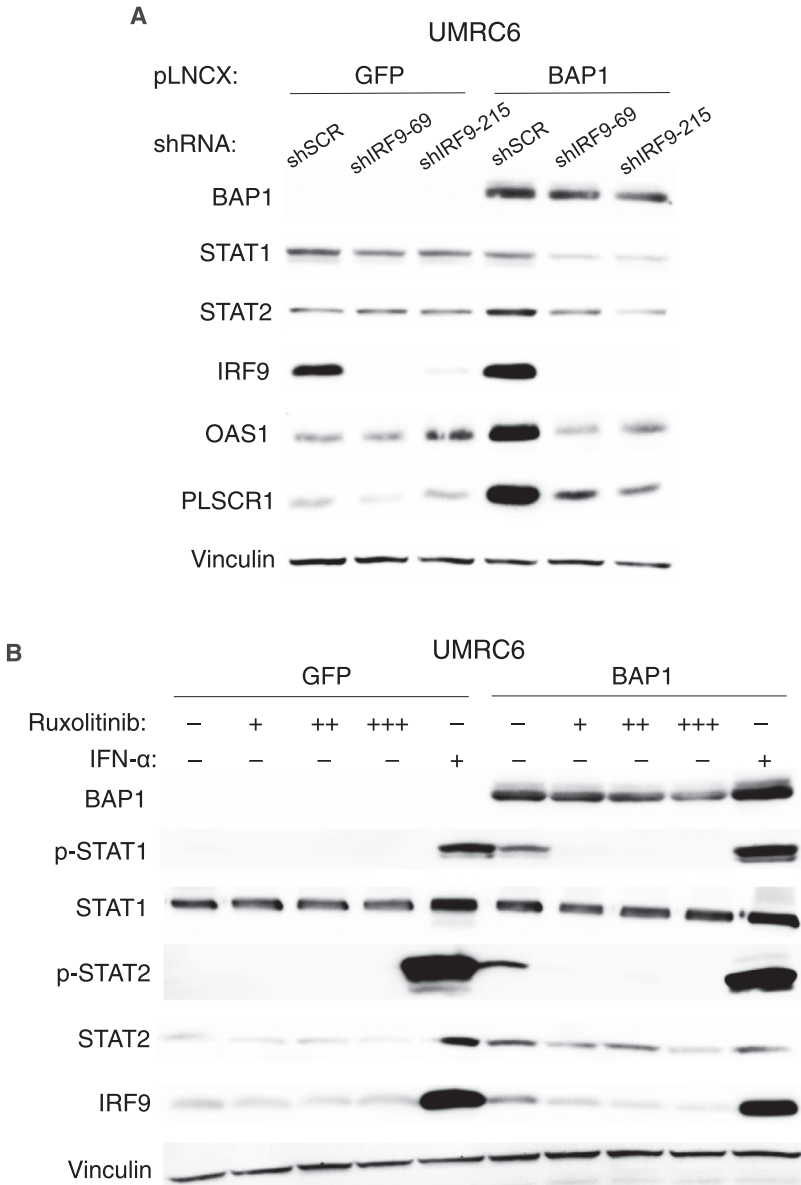
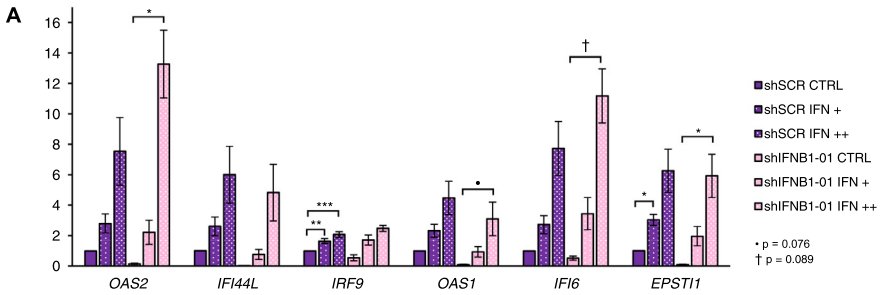
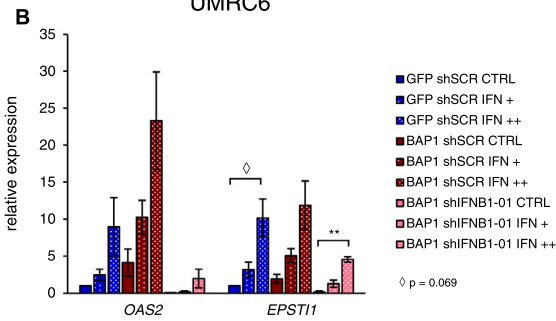


Fig. 1. ISGF3 activity is elevated in BAP1-expressing cells. **(A)** SDS-solubilized whole cell lysates of UMRC6 cells expressing GFP or a BAP1 construct and control (SCR) or IRF9 shRNAs and blotted with the indicated antibodies (n=3). **(B)** SDS-solubilized whole cell lysates of UMRC6 cells expressing GFP or a BAP1 construct, treated with the indicated concentrations of ruxolitinib or IFN- α 2 (2000 IU/ml) for 24 h, and blotted with the indicated antibodies (n=3). For ruxolitinib: +, 0.1 μ M; ++, 0.3 μ M; +++, 1 μ M.

Ren-02



UMRC6



UMRC6

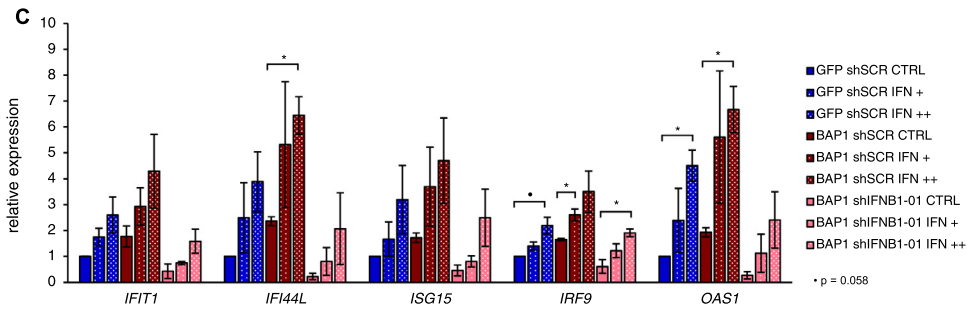


Fig. 2. IFN- β treatment increases ISGF3 target levels in *IFNB1* knockdown cells. (A) RT-qPCR measurement of the indicated transcripts in Ren-02 shSCR and shIFNB1-01 cells treated with CTRL (PBS) or IFN- β for 24 h ($n=2$). (B) RT-qPCR measurement of the indicated transcripts in UMRC6 GFP shSCR, BAP1 shSCR, and BAP1 shIFNB1-01 cells treated with CTRL (PBS) or IFN- β for 24 h ($n=2$). (C) RT-qPCR measurement of the indicated transcripts in UMRC6 GFP shSCR, BAP1 shSCR, and BAP1 shIFNB1-01 cells treated with CTRL (PBS) or IFN- β for 24 h ($n=2$). In all panels, t-tests were performed comparing the control to the IFN-treated within each cell line, and only comparisons with $p < 0.1$ are shown. IFN +, 25 pg/ml; IFN ++, 100 pg/ml.

2.3. *IFNAR1* knockdown reduces *ISGF3* target expression

Secreted IFN- β will need to bind to its receptor, IFNAR, at the plasma membrane to activate ISGF3. To further investigate the role of secreted IFN- β in BAP1-mediated ISGF3 activation, IFNAR1, a component of the interferon receptor, was suppressed by two shRNAs in UMRC6 GFP- and BAP1-expressing cells. IFNAR1 knockdown was confirmed by western blotting (Fig. 3A). In BAP1-expressing UMRC6 cells, IFNAR1 knockdown decreased ISGF3 target levels, as shown by

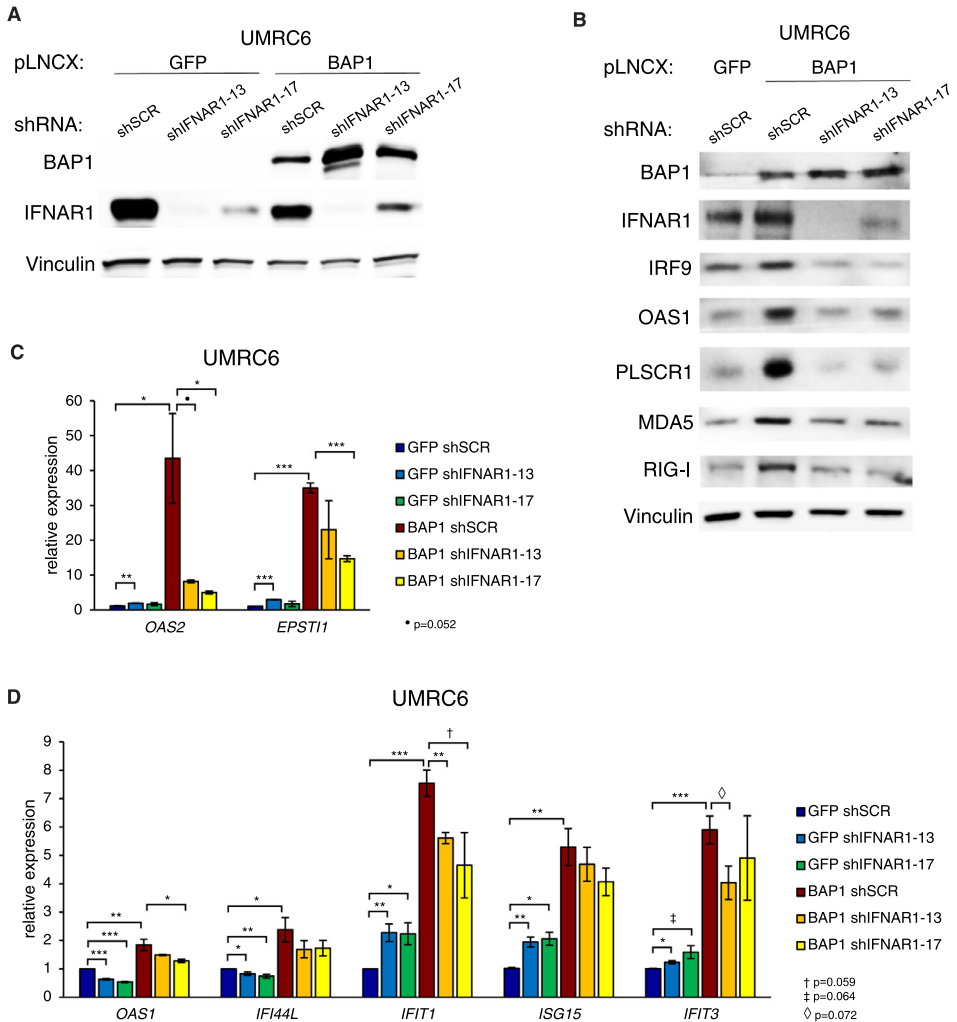


Fig. 3. IFNAR1 knockdown reduces ISGF3 target expression. (A) SDS-solubilized whole cell lysates of UMRC6 cells expressing control (GFP) or BAP1 constructs and control (SCR) or IFNAR1 shRNAs and blotted with the indicated antibodies (n=2). (B) SDS-solubilized whole cell lysates of UMRC6 cells expressing the indicated constructs and blotted with the indicated antibodies. (C, D) RT-qPCR measurement of the indicated transcripts in UMRC6 cells expressing control (GFP) or BAP1 constructs and control (SCR) or IFNAR1 shRNAs (n=3, n=4 for *OAS1*, *IFI44L*, *IFIT1*).

western blots of IRF9, OAS1, PLSCR1, MDA5, and RIG-I (Fig. 3B) and by qPCR of *OAS2*, *EPST11*, *OAS1*, *IFI44L*, *IFIT1*, *ISG15*, and *IFIT3* (Fig. 3C, D).

2.4. An IFN-β neutralizing antibody decreases ISGF3 target expression in BAP1-expressing cells

Our previous data suggest BAP1 enhances *IFNB1* expression to activate ISGF3 in ccRCC cells [1]. To assess whether secreted IFN-β leads to ISGF3 upregulation in these cells, BAP1-expressing cells were treated with increasing doses of an IFN-β neutralizing antibody, which binds secreted IFN-β in the media and prevents its binding to the IFNAR. After treatment, ISGF3 target expres-

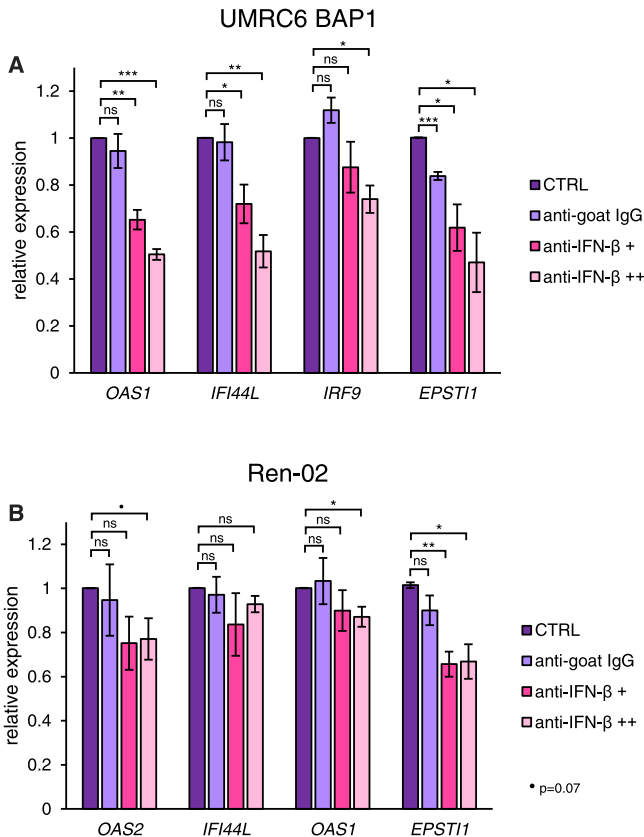


Fig. 4. An IFN- β neutralizing antibody decreases ISGF3 target expression in BAP1-expressing cells. (A) UMRC6 BAP1-expressing cells were treated with CTRL (PBS), anti-goat IgG (mock antibody treatment), or increasing doses of anti-IFN- β antibody for 5 days, and qPCR was performed on the indicated transcripts ($n=3$). (B) Ren-02 cells were treated with CTRL, anti-goat IgG, or increasing doses of anti-IFN- β antibody for 3 days, and qPCR was performed on the indicated transcripts ($n=3$). +, 0.1 $\mu\text{g/ml}$; ++, 0.2 $\mu\text{g/ml}$.

sion was measured by qPCR. Relative to untreated and control antibody-treated cells, anti-IFN- β treated cells had decreased expression of ISGF3 targets *OAS1*, *IFI44L*, *EPST11*, and others in UMRC6 BAP1-expressing cells (Fig. 4A) and Ren-02 cells (Fig. 4B).

2.5. Bap1 knockout reduces Sting levels in primary kidney cells from Bap1^{fl/fl} mice

We previously observed that BAP1 expression is associated with the expression of STING, an upstream stimulator of IFN production, in ccRCC cells. We sought to examine the impact of acute *Bap1* knockout on Sting protein levels in a different system using primary mouse kidney cells. Cells were isolated from the kidneys of WT and *Bap1*^{fl/fl} mice to form primary cultures. To characterize the cells, morphology was examined and immunohistochemistry was performed for cytokeratin 8, a marker of epithelial cells [3]. Many of the cultures had the morphology of epithelial cells (Fig. 5A). A cytokeratin 8 antibody stained epithelial cells in the normal mouse kidney, normal human kidney, human ccRCC, and the primary mouse cultured cells (Fig. 5B). To knock out Bap1, primary kidney cells from both WT and *Bap1*^{fl/fl} mice were treated with control virus or adeno-Cre virus. Western blot analyses of the protein lysates showed that Cre treatment

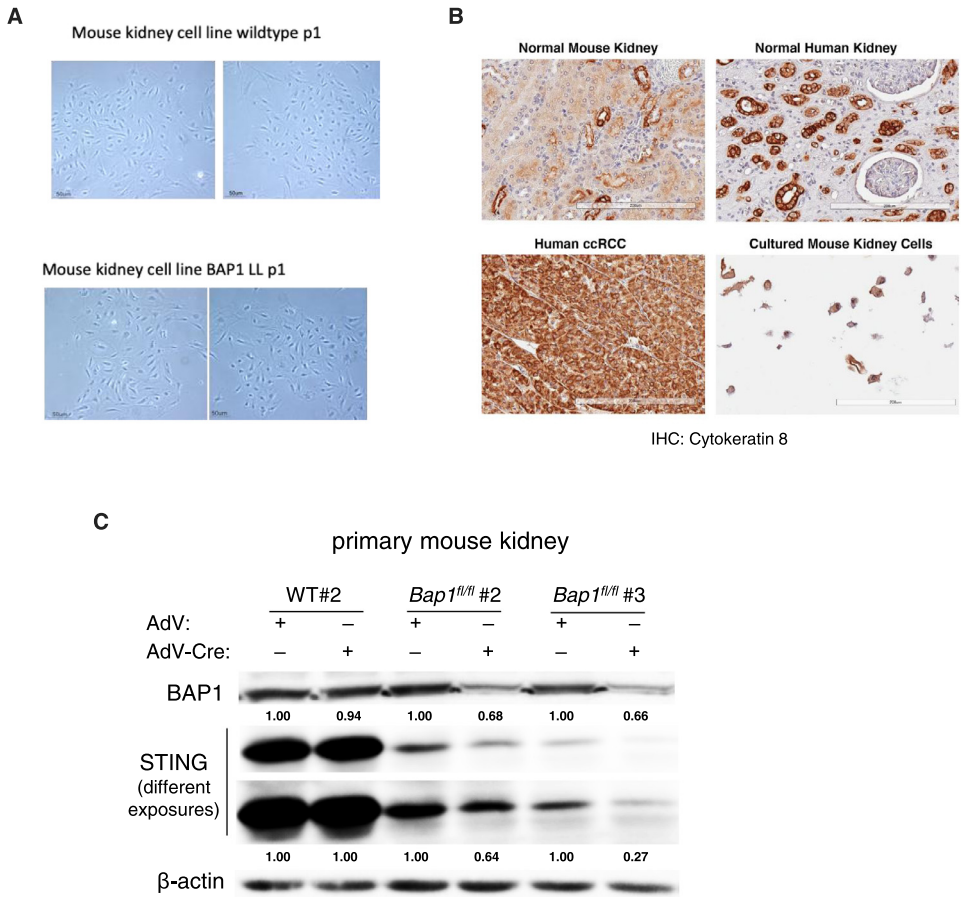


Fig. 5. *Bap1* knockout reduces STING protein levels in primary kidney cells from *Bap1^{fl/fl}* mice. **(A)** Phase contrast images of WT and *Bap1^{fl/fl}* mouse primary kidney cells. **(B)** Cytokeratin 8 immunohistochemistry performed on normal mouse kidney, normal human kidney, ccRCC and WT mouse primary kidney cells. **(C)** EBC-solubilized lysates of primary kidney cells from WT or *Bap1^{fl/fl}* mice treated with control or Cre adenovirus and blotted with the indicated antibodies.

reduced *Bap1* protein levels specifically in the *Bap1^{fl/fl}* cells. Further, *Sting* protein expression was decreased only in the Cre-treated *Bap1^{fl/fl}* cells (Fig. 5C).

2.6. *STING* knockdown reduces *ISGF3* target expression

To determine the impact of *STING* expression on *ISGF3* activity in ccRCC cells, *STING* was suppressed by shRNA in Ren-02 and UMRC6 GFP- and BAP1-expressing cells. Cells infected with *STING* shRNA demonstrated reduced *STING* protein levels. In Ren-02 cells, *STING* knockdown reduced the levels of *ISGF3* targets IRF9, OAS1, PLSCR1, and RIG-I (Fig. 6A). In UMRC6 cells, BAP1 re-expression increased the levels of *ISGF3* targets IRF9 and OAS1, and *STING* knockdown reversed this upregulation (Fig. 6B).

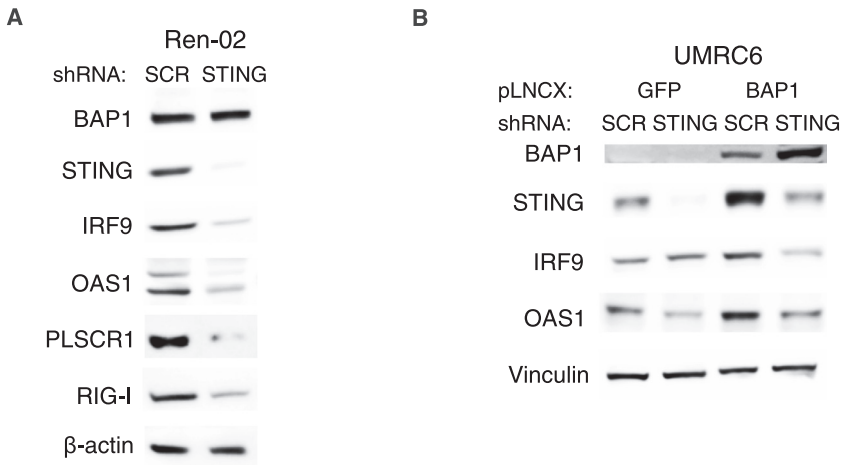


Fig. 6. STING knockdown reduces ISGF3 target expression. **(A)** EBC-solubilized lysates from Ren-02 cells expressing control or STING shRNA and blotted with the indicated antibodies (n=3). **(B)** EBC-solubilized lysates from UMRC6 cells expressing GFP or BAP1 and control or STING shRNA and blotted with the indicated antibodies (n=2).

2.7. A STING agonist increases CD45⁺ immune cells in BAP1-deficient xenografted tumors

As STING promotes ISGF3 activity, we sought to identify the biological impact of STING activation on tumor vasculature and tumor infiltrating immune cells in a ccRCC xenograft model. Ren-02 BAP1 knockdown cells were implanted subcutaneously in nude mice. Following tumor formation, mice were treated with vehicle or diABZI, a STING agonist, twice weekly via intraperitoneal injection. Immunohistochemistry was performed on the excised tumors from two pairs of mice. No major differences in CD31 staining (marker of tumor vasculature) were observed between conditions. CD45 staining (marker of tumor infiltrating immune cells), however, was elevated in the diABZI treated tumors (Fig. 7).

3. Experimental Design, Materials and Methods

3.1. Cell culture

UMRC6 cells were a gift from Qing Zhang. Ren-02 cells were a gift from Daniel Lindner. ccRCC cell lines were cultured in DMEM containing 10% FBS and 1% penicillin/streptomycin and maintained in 37 °C incubators with 5% CO₂. Stable cell lines were generated by lentiviral transduction. For knockdown cells, HEK293T cells were transfected with 2 μg ΔR8.9 packaging plasmid, 200 ng VSV-G envelope plasmid, and 2 μg pLKO shRNA plasmid using lipofectamine 2000. Viral supernatant was filtered and used to infect target cells overnight with 8 μg/ml polybrene. Infected cells were expanded and selected with 2 μg/ml puromycin for 4–7 days, until cells in an uninfected control plate died. For the STING knockdown cells, shSTING lentiviral particles were purchased from Santa Cruz (sc-92042-V) and used to infect cells following the manufacturer's protocol. The shRNA sequences are as follows: SCR: GCGCGUUUGUAGGAUUCGTT, IRF9-69: GCCATACTCCAGAATCTTA, IRF9-215: CTCAGTAGTTGTCCTGATAA, IFNB1-01: CCTACAAAGAAGCAGCAATTT, IFNAR1-13: GCCAAGATTCAGGAAATTATT, IFNAR1-17: GTTGACTCATTACACCATTT. For overexpression cells, phoenix cells were transfected with 2 μg pLNCX plasmid and lipofectamine 2000. The subcloning of BAP1 into pLNCX is described in our primary manuscript [1]. Viral supernatant was filtered and used to infect target cells overnight with 8 μg/ml polybrene. Infected cells were expanded and selected with 1 mg/ml G418 for 7–14 days,

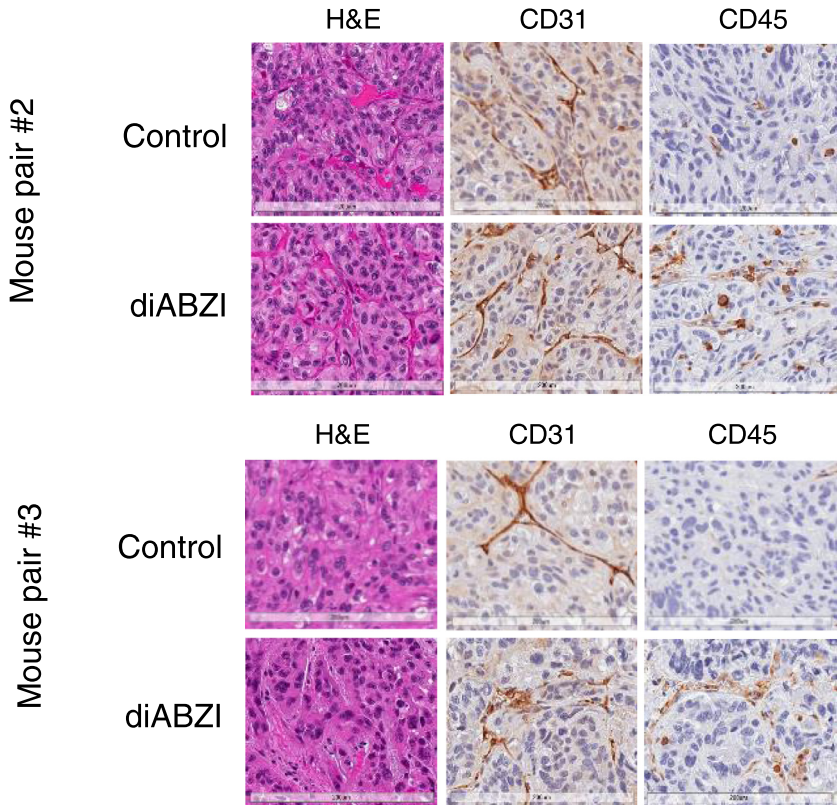


Fig. 7. A STING agonist increases CD45⁺ immune cell presence in BAP1-deficient xenografted tumors. H&E and IHC staining of tumor tissue from representative mice bearing Ren-02 shBAP1-74 xenografted tumors and treated with vehicle (control) or diABZI.

until cells in an uninfected control plate died. The generation of mouse primary kidney cells is described in detail in our primary manuscript [1].

3.2. Reagents

Antibodies for IFN- β and goat IgG were purchased from R&D Systems (AG814-SP and AB-108-C, respectively). Ruxolitinib was purchased from LC Laboratories (R-6688), IFN- β from R&D Systems (8499-IF), IFN- α 2B from R&D Systems (11013-IF), and diABZI from Med Chem Express (2138299-34-8).

3.3. Western blot analysis

Protein lysates were prepared using EBC buffer (120 mM NaCl, 50 mM Tris-HCl pH 8.0, 0.5% NP-40) or 1% SDS with 3×15 s sonication at 20 A. Lysates were boiled with 5X loading buffer for 10 min. Proteins were resolved by SDS-PAGE, transferred onto nitrocellulose membranes, blocked with 5% milk, and incubated with primary antibodies overnight. Membranes were washed 3×10 min with TBS-T, incubated with secondary antibodies, washed again with TBS-T, and developed on the ImageQuant LAS 4000 using Immobilon Western Chemilumines-

cent HRP substrates (Millipore Sigma, WBKLS0500). The antibodies and dilutions used are as follows: BAP1 (Santa Cruz sc-28383, 1:200), STAT1 (Cell Signaling Technology 9172S, 1:1000), STAT2 (Bethyl A303-512-A, 1:1000), IRF9 (Cell Signaling Technology 76684S, 1:1000), OAS1 (Cell Signaling Technology 14498S, 1:1000), PLSCR1 (Santa Cruz sc-59645, 1:200), p-STAT1 (Cell Signaling Technology 9171L, 1:1000), p-STAT2 (Cell Signaling Technology 88410, 1:1000), Vinculin (Santa Cruz sc-73614, 1:1000), IFNAR1 (Bethyl A304-290A-T, 1:1000), MDA5 (Cell Signaling Technology 5321S, 1:1000), RIG-I (Cell Signaling Technology 3743S, 1:1000), β -actin (Santa Cruz sc-8432, 1:200), STING (Cell Signaling Technology 13647S, 1:1000), anti-mouse IgG (Invitrogen 62-6520, 1:5000), and anti-rabbit IgG (Invitrogen 31460, 1:5000) [1].

3.4. qPCR

RNA was isolated from cells using the Qiagen RNeasy Mini Kit with QIAshredder columns and reverse transcribed using the Invitrogen SuperScript IV VILO master mix or Origene First Strand cDNA synthesis kit, all according to manufacturers' protocols. cDNA was diluted 1:10 and qPCR was performed using Power Track SYBR Green Master Mix on the StepOnePlus or QuantStudio 3 Real-Time PCR System. Initial denaturation was performed at 95 °C for 10 min followed by 40 cycles of 95 °C denaturation (15 s) and 60 °C annealing (60 s). The $\Delta\Delta$ Ct method was used to calculate relative gene expression. The following primers were used: IRF9-F: GCCCTACAAGGTGTATCAGTTG, IRF9-R: TGCTGTCGCTTTGATG-TGACT, IFIT1-F: AGAAGCAGGCAATCACAGAAAA, IFIT1-R: CTGAAACCGACCATAGTGGAAT, ISG15-F: CGCAGATCACCCAGAAGATCG, ISG15-R: TTCGTCGCATTTGTCCACCA, IFIT3-F: AAAAGCCCAACAAC-CCAGAAT, IFIT3-R: CGTATTGGTTATCAGGACTCAGC, OAS2-F: CAGTCCTGGTGAGTTGTCAGT, OAS2-R: ACAGCGAGGGTAAATCCTTGA, OAS1-F: TGTCCAAGGTGGTAAAGGGTG, OAS1-R: CCGCGATTAACT-GATCCTG, IFI44L-F: GAGCACAGAAATAGGCTTCTAGC, IFI44L-R: TGGTATCAGACCCCACTACGG, IFI6-F: GGTCTGCGATCCTGAATGGG, IFI6-R: TCACTATCGAGATACTTGTGGGT, EPST11-F: ACCCGCAATA-GAGTGGTGAAC, EPST11-R: GCTATCAAGGTGTATGCACCTTGT, GAPDH-F: ACCCACTCTCCACCTTTGA, GAPDH-R: CTGTTGCTGTAGCCAAATTCGT.

3.5. Immunohistochemistry

Xenografted Ren-02 BAP1 knockdown tumors were excised from mice treated with vehicle (40% PEG-400, 0.9% NaCl, 10% DMSO, filtered) or diABZI (3 mg/kg) twice weekly for 3.5–5 weeks via intraperitoneal injection. Tumors were formalin-fixed and paraffin-embedded, and immunohistochemistry was performed as described in our primary manuscript using the IntelliPATH FLX Autostainer and DAB substrate (DAKO, K3468) [1]. The following antibodies were used at the indicated dilutions: CD31 (Santa Cruz sc-1506, 1:500), CD45 (BD Pharmingen 550539, 1:200), Cytokeratin 8 (Abcam ab53280, 1:100), biotinylated anti-rabbit (Vector Laboratories BA-1000), biotinylated anti-rat (Vector Laboratories BA-4001).

3.6. Statistical analysis

Data are plotted as mean \pm SEM. Comparisons between conditions were performed using the two-tailed Student's t-test. Statistical significance is denoted in the figures as follows: * $p < 0.05$; ** $p < 0.01$; *** $p < 0.001$. Experiments were performed a minimum of two times.

Ethics Statements

Animal experiments were performed in accordance with ARRIVE guidelines and the NIH Guide for the Care and Use of Laboratory Animals. Protocol 01462 was approved by the Insti-

tutional Animal Care and Use Committee of Thomas Jefferson University. Male nude mice were used in xenograft experiments.

Declaration of Competing Interest

The authors declare that they have no known competing financial interests or personal relationships that could have appeared to influence the work reported in this paper.

Data Availability

Data supporting the roles of BAP1, STING, and IFN- β in ISGF3 activation in ccRCC (Original data) (Mendeley Data).

CRedit Author Statement

Lauren E. Langbein: Investigation, Formal analysis, Visualization, Writing – original draft; **Eleonora Sementino:** Investigation; **Zhijiu Zhong:** Investigation; **Wei Jiang:** Investigation; **Li Li:** Investigation; **Joseph R. Testa:** Resources, Writing – review & editing, Supervision, Funding acquisition; **Haifeng Yang:** Conceptualization, Resources, Writing – review & editing, Supervision, Funding acquisition.

Acknowledgments

Funding: This work was supported by the National Institutes of Health [5R01CA155015], Department of Defense Kidney Cancer Research Program [KC200248], Kidney Cancer Association, Kidney Cancer Research Alliance, and VHL Alliance, awarded to HY, as well as the Pennsylvania Department of Health and the International Association of Heat and Frost Insulators and Allied Workers, awarded to JRT. This work was also supported by the Translational Pathology Shared Resources of the Sidney Kimmel Cancer Center (SKCC), funded by NCI 5P30CA056036.

References

- [1] L.E. Langbein, R. El Hajjar, S. He, E. Sementino, Z. Zhong, W. Jiang, B.E. Leiby, L. Li, R.G. Uzzo, J.R. Testa, H. Yang, BAP1 maintains HIF-dependent interferon beta induction to suppress tumor growth in clear cell renal cell carcinoma, *Cancer Lett.* 547 (2022), doi:[10.1016/j.canlet.2022.215885](https://doi.org/10.1016/j.canlet.2022.215885).
- [2] L. Liao, Z.Z. Liu, L. Langbein, W. Cai, E.A. Cho, J. Na, X. Niu, W. Jiang, Z. Zhong, W.L. Cai, G. Jagannathan, E. Dulaimi, J.R. Testa, R.G. Uzzo, Y. Wang, G.R. Stark, J. Sun, S. Peiper, Y. Xu, Q. Yan, H. Yang, Multiple tumor suppressors regulate a HIF-dependent negative feedback loop via ISGF3 in human clear cell renal cancer, *eLife* (2018), doi:[10.7554/eLife.37925](https://doi.org/10.7554/eLife.37925).
- [3] S. Kanda, M. Ohmuraya, H. Akagawa, S. Horita, Y. Yoshida, N. Kaneko, N. Sugawara, K. Ishizuka, K. Miura, Y. Harita, T. Yamamoto, A. Oka, K. Araki, T. Furukawa, M. Hattori, Deletion in the cobalamin synthetase W domain-containing protein 1 gene is associated with congenital anomalies of the kidney and urinary tract, *J. Am. Soc. Nephrol.* 31 (1) (2020) 139–147, doi:[10.1681/asn.2019040398](https://doi.org/10.1681/asn.2019040398).